Desalination and Water Treatment
www.deswater.com

doi:10.5004/dwt.2018.22200

111 (2018) 278–285
April

Adsorptive removal of Pb(II) metal from aqueous medium using biogenically synthesized and magnetically recoverable core-shell structured AM@Cu/Fe_3O_4 nano composite

K. Deepa[a], Cheera Prasad[a], N.V.V. Jyothi[a,*], Mu. Naushad[b,*], Saravanan Rajendran[c], S. Karlapudi[a], S. Himagirish Kumar[a]

[a]*Department of Chemistry, S.V. University, Tirupati, Andhrapradesh, India, email: nvvjyothi01@gmail.com (N.V.V. Jyothi)*
[b]*Department of Chemistry, College of Science, Bld#5, King Saud University, Riyadh-11451, Saudi Arabia, email: shad81@rediffmail.com (M. Naushad)*
[c]*Escuela Universitaria de Ingeniería Mecánica (EUDIM), Universidad de Tarapacá, Avda. General Velásquez 1775, Arica, Chile*

Received 14 January 2018; Accepted12 March 2018

ABSTRACT

Herein, we have reported an eco-friendly and facile scheme for the synthesis of copper nano particles supported iron oxide magnetic nano particles(Cu/Fe_3O_4 MNPs) using the extract of *Aeglemarmelos (AM)* leaves as a reducing and capping agent. The synthesized material (AM@Cu/Fe_3O_4 nano composite) was characterized by various techniques. The results showed that AM@Cu/Fe_3O_4 MNP had good specific surface area (27.36 m^2/g) and agglomerated spherical in shape with the size range 16–20 nm. The magnetic properties of AM@Cu/Fe_3O_4 MNPs sample clearly showed ferromagnetic nature with a saturation magnetization (Ms) of 25.2 emu/g. Besides, AM@Cu/Fe_3O_4 magnetic nano composite was applied for the removal of Pb (II) from aqueous medium. The adsorption process was studied at contact time, pH and various concentrations. The adsorption data was fitted using Freundlich and Langmuir models. The kinetic results showed that adsorption was followed the pseudo-second-order kinetic model.

Keywords: Nano composite; Leaves extract; Biogenic; Toxic metal; Adsorption

1. Introduction

Recently, nano materials have become attractive sorbent materials because of their high surface, abundant functional groups and enhanced activity sites on the surface than bulk materials [1,2]. Some nano materials have been functionalized with various chemical groups to enhance their affinity for target compounds [3–6]. Especially, iron oxide nano particles have shown pronounced interest because these have the applications in magnetic resonance imaging [7], spintronics [8,9], lithium ion battery field [10], catalysis [11,12], targeted drug delivery [13,14] and environmental remediation [15–24]. Binary metal nano particles offer prospective applications in the fields of biomedicine and heterogeneous catalysis, nano technology and environmental science [25–27]. The preparation of bimetallic nano particles by using plant extracts is economical, safe, biocompatible and eco-friendly method. There are still few reports available on the biogenic synthesis of metal/iron oxide nano particles (NPs) [28–30] and also a few of the nano particles are of high cost. So, we have preferred a facile and biogenic synthesis of Cu/Fe_3O_4 MNPs by using *Aeglemarmelos* leaves extract as the capping and reducing agent. Moreover, the prepared AM@Cu/Fe_3O_4 nano composite was used for the removal of Pb (II) metal ion from aqueous solutions which is one of the most toxic heavy metal ions [31]. There are several metals which are toxic like arsenic, copper, nickel, cadmium, mercury, chromium and lead because these metal are non-degradable and accumulates in the living organisms [32–37]. Several techniques such as electro deposition, ion-exchange,

*Corresponding author.

photo catalysis, chemical coagulation, extraction, membrane separation, chemical precipitation, and adsorption have been applied for the removal of toxic metal ions from aqueous medium [38–41]. The heavy metals are not eco-friendly and be liable to accrue in living organisms causing foremost health problem [42–44]. Thus,the removal of metal ions from aqueous system is extremely important and has become a demanding task for scientists [45].

2. Materials and methods

2.1. Instruments and reagents

Ferric chloride hexa hydrate, sodium acetate, HCl, NaOH, $(CH_3COO)_2Pb{\cdot}3H_2O$ and $CuCl_2{\cdot}2H_2O$ were purchased from Sigma Aldrich, India. The *Aeglemarmelos* (bael) leaves were collected around the Tirupati located in A.P., India. The phase purities of prepared nano particles was checked by X-ray diffraction (XRD) technique (Seifert 3003 TT X-ray diffract meter with Cu Kα radiation with a wavelength of 1.52 Å).The size and shape of the nano particle range was determined by TEM which was carried out with a JEOL JEM-3010 instrument and the quantitative elemental analysis of AM@Cu/Fe_3O_4 MNPs was carried out on Oxford instruments Inca Penta FET × 3 Energy Dispersive Spectrum (EDS).

2.2. Preparation of aeglemarmelos leaves(AM) extract

*Aeglemarmelos (*Bael) leaves were collected around the Tirupati, India. Then, they were crushed into fine powder using motor and pestle. An intense green coloured extract of *Aeglemarmelos* was extracted which was used in the present study.

2.3. Preparation of the copper nano particles

In a 250 mL conical flask, 100 mL of the *Aeglemarmelos* leaves extract and 50 mL of 5 mM $CuCl_2{\cdot}2H_2O$ solution were shaken vigorously until the color changed into dark brown which is the indication of the formation of Cu NPs suspension.

2.4. Preparation of the AM@Cu/Fe_3O_4 magnetic nanoadsorbent

In a 250 mL conical flask, 40 mL leaves extract of the *Aeglemarmelos*, 0.3 g $CuCl_2{\cdot}2H_2O$ and 1.0 g $FeCl_3{\cdot}6H_2O$ were taken which were mixed in 50 mL of milli-Q water and stirred for 2 h at 50°C by adjusted pH using 1 M HCl/NaOH solution. After the completion of stirring the mixture,the color was gradually changed in to dark brown as Cu/Fe_3O_4 nano particles were formed.

2.5. Batch adsorption experiments

The adsorption of Pb (II) ion using AM@Cu/Fe_3O_4 MNPs was studied by batch methods with pH range varied from 2 to 7 at 301K. 3.5 mg of AM@Cu/Fe_3O_4 MNPs was shaken with 25 mL of Pb (II) ion solution of known concentration in the Erlenmeyer's flask. The pH of the solution was set using 0.1 M HCl/NaOH solution. After the equilibration time, the magnetic nano adsorbent was separated magnetically from the above solution. The concentration of Pb (II) ions in the solution phase was determined using FAAS (Shimadzu AA-6300). All the sorption experiments were done in three replicates and the average value was taken. The amount of Pb (II) adsorbed by the AM@Cu/Fe_3O_4 MNPs at equilibrium (q_e) was evaluated as:

$$q_e = \frac{(C_i - C_e)V}{M} \tag{1}$$

The percent adsorption was defined as:

$$Adsorption(\%) = \frac{(C_i - C_e)}{C_i} \times 100 \tag{2}$$

3. Results and discussion

3.1. Characterization

Fig. 1 reveals the X-ray diffraction pattern (XRD) of the AM@Cu/Fe_3O_4MNPs. The diffraction peaks at 2θ; 30.04, 35.42, 43.05, 57.1 and 62.7 could be indexed to (220), (311), (400),(333) and (440) planes of cubic Fe_3O_4(JCPDS-82-1533) suggestive of the synthesis of Fe_3O_4 particles [46,47]. The peaks at 2θ values 43.175, 51.7 and 74.127 might be easily allotted to (111), (200) and (220) crystal planes in copper cubic structure which agrees with the standard copper (JCPDS 19-0629). Further, we have determined the crystallite size of Fe_3O_4 nano particles by Scherer equation:

$$D = \frac{0.89\lambda}{\beta\cos\theta} \tag{3}$$

where D is the average particle size, θ is the diffraction angle, λ is the wave length of the Cu-Kα irradiation and β is the full width at half maximum intensity of the diffrac-

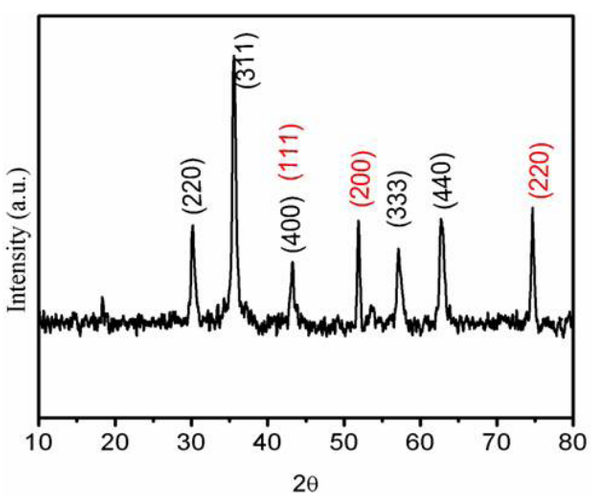

Fig. 1. The powder XRD pattern of the AM@Cu/ Fe_3O_4 MNPs sample.

tion peak. The calculated crystalline size for Fe_3O_4 particles was about ~36 nm which is in good agreement with TEM results.

The morphology and size of the AM@Cu/Fe_3O_4 MNPs were observed by TEM Fig. 2. This TEM image showed that the synthesized AM@Cu/Fe_3O_4MNPs were agglomerated in spherical shape and the particle size was ~16 to 20 nm. The results demonstrated that Cu NPs were attached to the surface of Fe_3O_4 which reveals a good bonding between Fe_3O_4 and Cu NPs. We have also applied EDS method for chemical composition of the AM@Cu/Fe_3O_4MNPs. Fig. 3 proved that the AM@Cu/Fe_3O_4 MNP had copper (Cu), oxygen (O) and iron (Fe). The EDS investigation showed that copper nano particles were decorated on the surface of Fe_3O_4 MNPs.

Fig. 4 reveals the porous nature of AM@Cu/Fe_3O_4 MNPs which was examined by N_2 adsorption-desorption method. The sample displayed the typical IV type of IUPAC classification of adsorption isotherms. The BET surface area of AM@Cu/Fe_3O_4 MNPs was found to be 27.36 m^2/g. The total pore volume and pore size distribution was studied by the Barret-Joyner-Halenda (BJH) analysis. The result indicated that AM@Cu/Fe_3O_4 had the total pore volume 0.136 cm^3/g and meso porous in nature with the pore size range from 12 to 26 nm.

The magnetic activities of the synthesized AM@Cu/Fe_3O_4 MNPs were investigated by using a vibrating sample magnetometer at room temperature, with the field sweeping from −20 to +20 kOe. As shown in Fig. 5, the saturated magnetization value of AM@Cu/Fe_3O_4 MNPs was 25.2 emu/g which demonstrated the ferromagnetic nature of the material. Hence, the nano composite could be easily separated by using an external magnetic field.

3.2. Adsorption studies

The effect of the pH on the exclusion of Pb (II) ion by AM@Cu/Fe_3O_4 MNPs was studied in the pH range 2–7 at the temperature: 301 K and Pb (II) concentrations: 25–45 mg/L. Fig. 6a shows that the adsorption process was

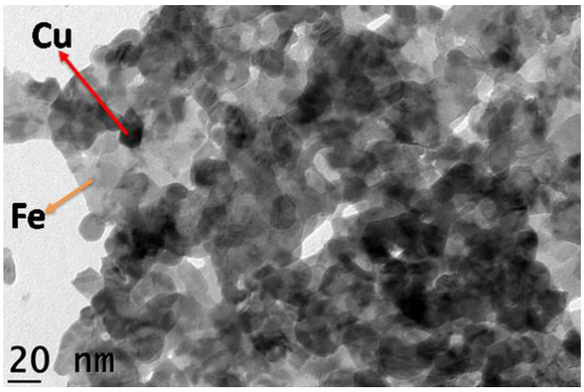

Fig. 2. Transmission electron microscope (TEM) image of synthesized AM@Cu/ Fe_3O_4 nano composite.

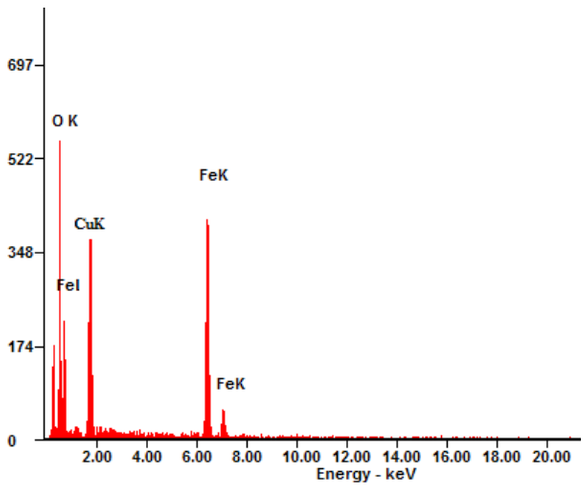

Fig. 3. Energy dispersive X-ray spectroscopy (EDX) image of synthesized AM@Cu/Fe_3O_4 MNPs.

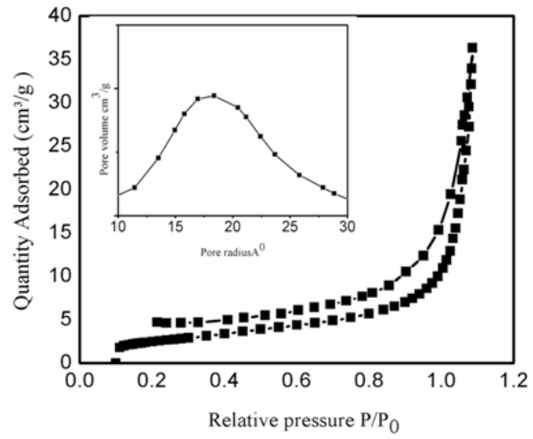

Fig. 4. N_2 adsorption-desorption isotherm for AM@Cu/Fe_3O_4 MNPs sample.

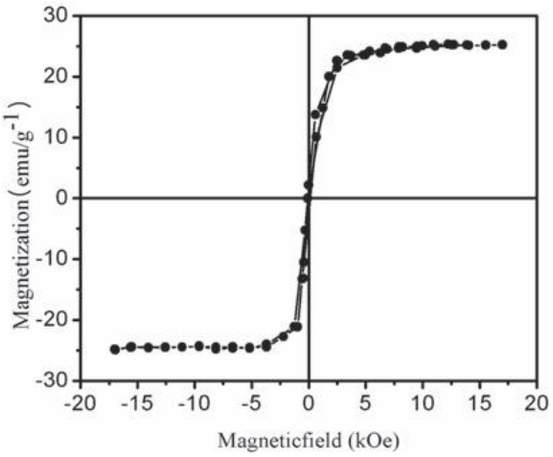

Fig. 5. M-H hysteresis curve of AM@Cu/ Fe_3O_4 MNPs sample measures at 301 K.

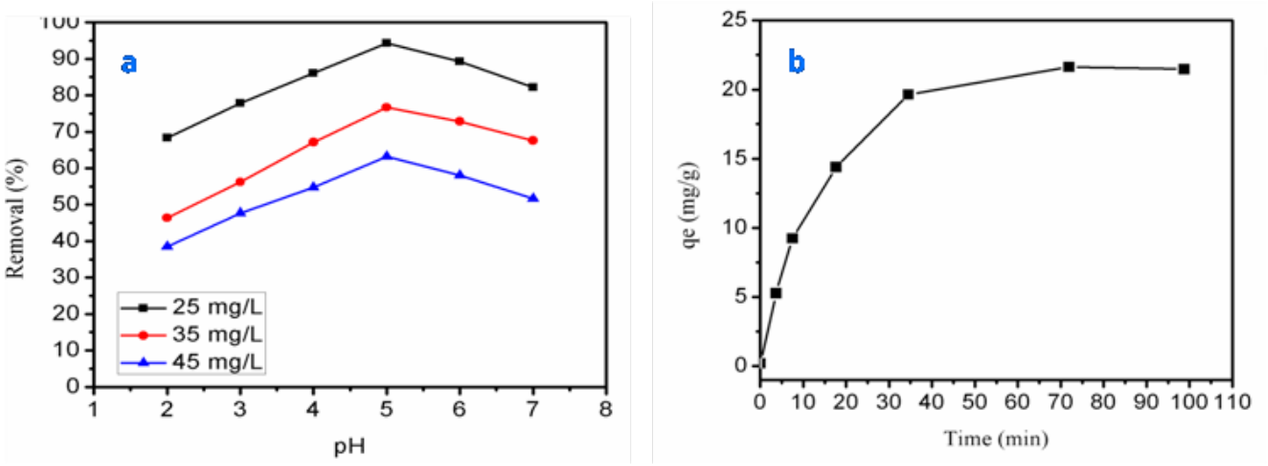

Fig. 6(a). Effect of pH (different initial concentration of Pb (II): 25, 35, 45 mg/L, solution volume: 25 mL, time: 120 min, temperature: 301 K) and (b) effect of contact time on the adsorption of Pb (II) by AM@Cu/Fe_3O_4 MNPs (initial concentration of Pb (II): 25 mg/L, solution volume: 25 mL, pH: 5, temperature: 301 K).

abruptly enhanced with the increase in pH from 2 to 5 and reduced with the further increase in pH from 6 to 7. The nano composite showed a maximum removal (95.48%) at pH 5.0 at the initial concentration of 25 mg/L. At the higher pH, the low percentage of Pb (II) removal was due to the formation of hydroxides of Pb (II)in the form of Pb $(OH)_3^-$, Pb $(OH)_2$and Pb $(OH)^+$ at different pH values [48]. At lower pH, the removal of Pb (II) was inhibited due to the H^+ competed with Pb (II) for sorption sites [49] which appreciably decreased Pb (II) sorption.

3.3. Adsorption kinetic studies

Fig. 6b shows that the adsorption of Pb(II) at pH: 5.0, temperature: 301 K, initial Pb (II) concentration: 25 mg/L at different time. The adsorption of the Pb (II) using AM@Cu/Fe_3O_4 MNPs was almost finished within 35 min and then gradually reached the equilibrium in 72 min. The pseudo first order [50] and pseudo second order [51] kinetic models were used to examine the kinetics for the removal Pb (II) using AM@Cu/Fe_3O_4MNPs nano composite. The linear form of these two kinetic models was explained by the subsequent equations:

$$\log\left(q_e - q_t\right) = \log q_e - \left(\frac{k_1}{2.303}\right)t \tag{4}$$

$$\frac{t}{q_t} = \frac{1}{k_2 q_e^{\,2}} + \left(\frac{1}{q_e}\right)t \tag{5}$$

It is clear from Table 1 that the values of correlation coefficient was better for pseudo second order kinetic model (> 0.998) which showed the better fitting of pseudo-second-order kinetics model.

3.4. Adsorption isotherms

In the present study, the isotherm results were analyzed using the Langmuir and Freundlich isotherms [52,53]. The linearized form of the Langmuir isotherm was represented as following equation:

$$\frac{C_e}{q_e} = \frac{C_e}{q_m} + \frac{1}{q_m\, b} \tag{6}$$

The values of q_m and b were found from the slope and intercept of C_e/q_e versus $1/C_e$ as mentioned in Table 2. The Langmuir isotherm dimension less separation factor (R_L) was defined by the following equation:

$$R_L = \frac{1}{1 + bC_i} \tag{7}$$

For the favorable adsorption, R_L value must lie within 0–1 and in our present study, the value of R_L was 0.0786 which indicated the favorable adsorption of Pb(II) onto AM@Cu/Fe_3O_4 MNPs. The linearized form of the Freundlich isotherm model is given as:

$$\log q_e = \log K_f + \frac{1}{n}\log C_e \tag{8}$$

The values of K_f and 1/n were obtained from the plots of log q_e vs. log C_e which are shown in Table 2. The Langmuir isotherm fitted quite well with the experimental data due to the better value of correlation coefficient (R^2 = 0.999) (Fig. 7).

Table 1
Kinetic parameters for the adsorption of Pb(II) onto AM@Cu/Fe_3O_4 MNPs at different metal ion concentrations

Conc. of Pb(II) (ppm)	Pseudo-first-order			Pseudo-second-order		
	K_1 (1/min)	R^2	SSE	K_2 (g/mg·min)	R^2	SSE
25	0.026	0.986	0.901	0.013	0.999	0.0171
35	0.029	0.976	0.904	0.016	0.999	0.0076
45	0.037	0.967	0.908	0.021	0.998	0.0082

Table 2
Langmuir and Freundlich isotherm constants and correlation coefficients for Pb (II) adsorption onto AM@Cu/ Fe_3O_4 MNPs at constant temperature

Temp. (K)	Langmuir				Freundlich			
	q_m (mg /g)	b (L/mg)	R^2	χ^2	K_f (mg /g)	$1/n$	R^2	χ^2
301	46.56	9.58	0.999	10.57	12.68	0.558	0.983	56.53

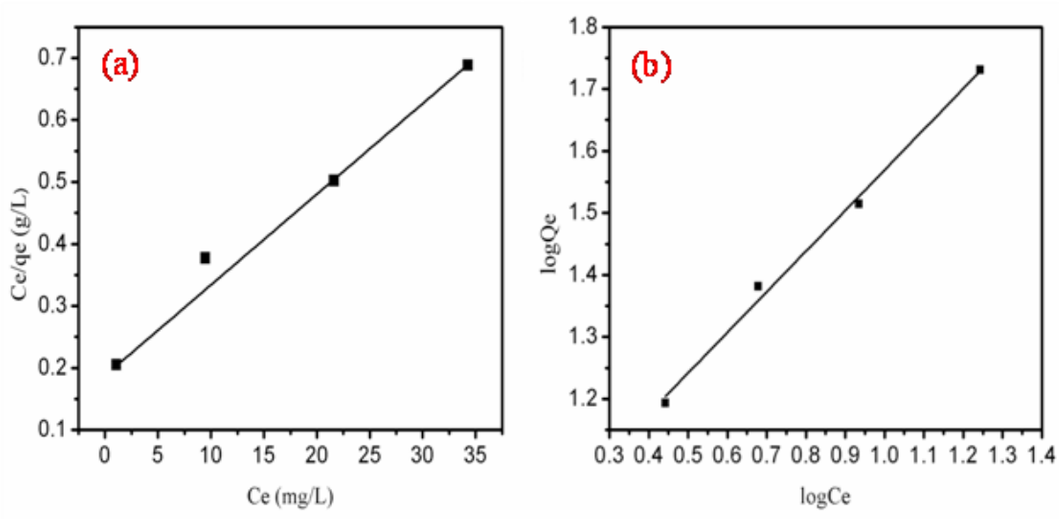

Fig. 7. Linear plot of (a) Langmuir and (b) Freundlich isotherm models.

Table 3 shows the list of comparison of maximum mono layer adsorption capacities for Pb (II) using different adsorbents [54–65]. It was noted that AM@Cu/Fe_3O_4 had better adsorption capacity in comparison to most of the other adsorbents. So, AM@Cu/Fe_3O_4 nano composite is a prospective material for the removal of Pb (II) from aqueous medium.

3.5. Desorption and reusability

It is desirable for any adsorbent to retain the adsorption capacity when regenerated to be reused further that makes the adsorbent economically viable. Therefore, the regeneration of AM@Cu/Fe_3O_4 MNPs was carried out using 0.2 M HCl that leads to the desorption of the Pb (II) from the adsorbent surface. The acidic pH favors the desorption of Pb (II) from the AM@Cu/Fe_3O_4 MNPs adsorbent. This is due to the fact that higher concentration of hydrogen ion makes the surface positively charge due to higher protonated groups that helps in desorption of positively charged Pb (II) ions. It is also evident from our pH studies that at low pH the adsorption capacity of AM@Cu/Fe_3O_4 MNPs was found to be low due to competition between H^+ and Pb (II) ions. This result also supports the greater desorption of Pb (II) at acidic pH. Further, the regenerated AM@Cu/Fe_3O_4 MNPs adsorbent was further tested for adsorption of Pb (II) to check the feasible re usability of the adsorbent. The results showed that the regenerated adsorbent showed 94, 88 and 80% removal for first, second and third cycle respec-

Table 3
Comparison of adsorption capacity of various adsorbents with AM@Cu/ Fe_3O_4 MNPs for the removal of Pb (II) ions

Adsorbent	q_{max} (mg/g)	References
ZVI-GAM	78.13	54
Magnetic chitosan/graphene oxide	76.94	55
Van apple pulp activated carbon	15.96	56
Fe_3O_4@C	71.42	57
Fe_3O_4/SiO_2 nanocomposite	17.65	58
Fe_3O_4 nanospheres	18.47	59
Chitosan-tripolyphosphate beads	57.33	60
Chitosan immobilized on bentonite	32.55	61
Ti(IV) iodovanadate	18.8	62
Ethylene diamine tetra acetic acid-Zr(IV) iodate	26.04	63
Polyaniline Sn(IV) tungstomolybdate	44.64	64
Sodium dodecyl sulfate acrylamide Zr(IV) selenite	18.38	65
AM@Cu/ Fe_3O_4MNPs	46.56	Present study

tively. This result indicated that AM@Cu/Fe_3O_4 MNPs is a promising adsorbent that can be regenerated and be reused.

4. Conclusion

In this work, we studied environmentally benign method for the biogenic synthesis of AM@Cu/Fe_3O_4 MNPs. The particles in synthesized nano composite were spherical in shape and were explored by transmission electron microscope. The powder XRD results confirmed the formation of AM@Cu/Fe_3O_4MNPs. The surface area of the AM@ Cu/Fe_3O_4 MNPs was studied by N_2 adsorption-desorption method. The magnetic properties of the synthesized AM@Cu/Fe_3O_4 MNPs were analyzed by using a VSM at 301 K.The maximum sorption capacity was estimated to be 46.56 mg/g at pH-5 and temperature 301 K. The sorption data was best fitted by Langmuir isotherms model and adsorption followed pseudo second order kinetic model. We have also found that the adsorbent could be easily separated by using external magnet. These characteristics of magnetically separable AM@Cu/Fe_3O_4MNPs make it an auspicious material for many environmental applications.

Acknowledgement

One of the authors, K. DEEPA extends her sincere thanks to UGC-New Delhi for providing financial support in the form of UGC-PDWF (No. F.15-1/2016-17/PDFWM-2015-17AND-35207 (SAII).

References

[1] M.R. Awual, M.M. Hasan, G.E. Eldesoky, M.A. Khaleque, M.M. Rahman, M. Naushad, Facile mercury detection and removal from aqueous media involving ligand impregnated conjugate nano materials, Chem. Eng. J., 290 (2016) 243–251.
[2] Z.A. ALOthman, M.M. Alam, Mu. Naushad, Heavy toxic metal ion exchange kinetics: Validation of ion exchange process of composite cation exchanger nylon 6,6 Zr(IV) phosphate, J. Ind. Eng. Chem., 19 (2013) 956–960.
[3] Y.L.F. Musico, C.M. Santos, M.L.P. Dalida, D.F. Rodrigues, Improved removal of lead (II) from water using a polymer-based graphene oxide nano composite, J. Mater. Chem. A., 1 (2013) 3789–3796.
[4] A.A. Alqadami, Mu. Naushad, M.A. Abdalla, M.R. Khan, Z.A. ALOthman, Adsorptive removal of toxic dye using Fe_3O_4–TSC nano composite: equilibrium, kinetic, and thermodynamic studies, J. Chem. Eng. Data, 61 (2016) 3806–3813.
[5] A.A. Alqadami, Mu. Naushad, M.A. Abdalla, T. Ahmad, Z.A. ALOthman, S.M. ALShehri, A.A. Ghfar, Efficient removal of toxic metal ions from wastewater using a recyclable nanocomposite: A study of adsorption parameters and interaction mechanism, J. Cleaner Production, 156 (2017) 426–436
[6] C. Prasad, P. KrishnaMurthy, R. HariKrishna, R. SreenivasaRao, V.Suneetha, P. Venkateswarlu, Bio-inspired green synthesis of RGO/Fe_3O_4 magnetic nano particles using Murrayakoenigii leaves extract and its application for removal of Pb (II) from aqueous solution, J. Environ. Chem. Eng., 5 (2017) 4374–4380.
[7] S. Xuan, F. Wang, J.M.Y. Lai, K.W.Y. Sham, Yi.X.J. Wang, S.F. Lee, J.C. Yu, C.H.K. Cheng, K.C.F. Leung, Synthesis of biocompatible, mesoporous Fe_3O_4 nano/micro spheres with large surface area for magnetic resonance imaging and therapeutic applications, Appl. Mater. Interfaces, 3 (2011) 237–244.
[8] D.H. Zhang, Z.Q. Liu, S. Han, Magnetite (Fe_3O_4) core shell nano wires: synthesis and magneto resistance, Nano Lett., 4 (2004) 2151–2155.
[9] Y.Q. Zhan, R. Zhao, Y.J. Lei, F.B. Meng, J.C. Zhong, X.B. Liu, A novel carbon nanotubes/Fe_3O_4 inorganic hybrid material: synthesis, characterization and microwave electromagnetic properties, J. Magn. Magn. Mater., 323 (2011) 1006–1010.
[10] J.S. Xu, Y.J. Zhu, Monodisperse Fe_3O_4 and c-Fe_2O_3 magnetic mesoporous micro spheres as anode materials for lithium-ion batteries, Appl. Mater. Interfaces, 4 (2012) 4752–4757.
[11] A.H. Lu, W. Schmidt, N. Matoussevitch, H. Bonnemann, B. Spliethoff, B. Tesche, E. Bill, W. Kiefer, F. Schuth, Nano engineering of a magnetically separable hydrogenation catalyst, Angew. Chem. Int. Ed., 43 (2004) 4303–4306.
[12] C. Prasad, S. Gangadhara, P. Venkateswarlu, Bio-inspired green synthesis of Fe_3O_4 magnetic nano particles using watermelon rinds and their catalytic activity, Appl Nano sci., 6 (2016) 797–802.
[13] Y. Zhu, Y. Fang, S. Kaskel, Folate-conjugated Fe_3O_4@SiO_2 hollow mesoporous spheres for targeted anticancer drug delivery, J. Phys. Chem. C., 114 (2010) 16382–16388.
[14] Y. Chen, H. Chen, D. Zeng, Y. Tian, F. Chen, J. Feng, J. Shi, Core/shell structured hollow meso porous nano capsules: a potential platform for simultaneous cell imaging and anticancer drug delivery, ACS Nano. 4 (2010) 6001–6013.
[15] S. Linley, T. Leshuk, F.X. Gu, Synthesis of magnetic rattle type nano structures for use in water treatment, Appl. Mater. Interfaces, 5 (2013) 2540–2548.
[16] Y. Liu, Y. Wang, S. Zhou, S. Lou, L. Yuan, T. Gao, X. Wu, X. Shi, K. Wang, Synthesis of high saturation magnetization super paramagnetic Fe_3O_4 hollow micro spheres for swift chromium removal, Appl Mater. Interfaces, 4 (2012) 4913–4920.
[17] Q. Cheng, F. Qu, N.B. Li, H.Q. Luo, Mixed hemi micelles solid-phase extraction of chlorophenols in environmental water samples with 1-hexadecyl-3-methylimidazolium bromide-coated Fe_3O_4 magnetic nano particles with high-performance liquid chromatographic analysis, Anal. Chim. Acta, 715 (2012) 113–119.
[18] C. Prasad, S. Karlapudi, G. Sellola, V. Ponneri, A facile green synthesis of spherical Fe_3O_4 magnetic nano particles and their effect on degradation of methylene blue in aqueous solution, Journal of Molecular Liquids, 221 (2016) 993–998.
[19] C. Prasad S. Karlapudi, G. Sellola, P. Venkateswarlu, Bio inspired green synthesis of Ni/Fe_3O_4 magnetic nano particles using *Moringa oleifera* leaves extract: A magnetically recoverable catalyst for organic dye degradation in aqueous solution, Journal of Alloys and Compouds, 700 (2017) 252–258.
[20] C. Prasad, G. Yuvaraja, P. Venkateswarlu, Biogenic synthesis of Fe_3O_4 magnetic nanoparticles using Pisum sativum peels extract and its effect on magnetic and Methyl orange dye degradation studies, J.Magn.Magn. Mater. 424 (2017) 376–381.
[21] C. Prasad, S. Karlapudi, P. Venkateswarlu, I. Bahadur, S. Kumar, Green arbitrated synthesis of Fe_3O_4 magnetic nano particles with nano rod structure from pomegranate leaves and Congo red dye degradation studies for water treatment, J. Molec. Liq., 240 (2017) 322–328
[22] C. Prasad , S. Karlapudi , C. Narasimha Rao, P. Venkateswarlu, I. Bahadur , A highly resourceful magnetically separable magnetic nano particles from aqueous peel extract of Bottle gourds for organic dyes degradation, J. Molec. Liq., 243 (2017) 611–615.
[23] C Prasad, K Srinivasulu, P Venkateswarlu, Catalytic reduction of 4-nitrophenol using biogenic silver nano particles derived from papaya (Carica papaya) peel extract, Ind. Chem., 1 (2015) 1–4.
[24] S. Karlapudi, C. Prasad, S.H. Kumar, N.V.V. Jyothi, P. Venkateswarlu, Bio inspired green synthesis of Fe_3O_4 magnetic nano particles using Cassia occidentalis leaves extract and efficient catalytic activity for degradation of 4-nitro phenol, Pharmacia Lettre., 10 (1) (2018) 55–62.
[25] N.R. Kim, K. Shin, I. Jung, M. Shim, H.M. Lee, Ag–Cu bimetallic nano particles with enhanced resistance to oxidation: a combined experimental and theoretical study, J. Phys. Chem., C. 118 (2014) 26324–26331.

[26] N. Moghimi, M. Mohapatra, K.T. Leung, Bimetallic nano particles for arsenic detection, Anal. Chem., 87 (2015) 5546–5552.
[27] S.M. Roopan, T.V. Surendra, G. Elango, S.H.S. Kumar, Biosynthetic trends and future aspects of bimetallic nano particles and its medicinal applications, bio synthetic trends and future aspects of bimetallic nano particles and its medicinal applications, Appl. Microbiol. Biotechnol., 98 (2014) 5289–5300.
[28] S.S. Momeni, M. Nasrollahzadeh, A. Rustaiyan, Green synthesis of the Cu/ZnO nano particles mediated by Euphorbia prolifera leaf extract and investigation of their catalytic activity, J. Colloid Interface Sci., 472 (2016) 173–179.
[29] S.M. Sajadi, M. Nasrollahzadeh, M. Maham, Aqueous extract from seeds of Silybummarianum L. as a green material for preparation of the Cu/Fe_3O_4 nano particles: A magnetically recoverable and reusable catalyst for the reduction of nitro arenes, J. Colloid Interface Sci., 469 (2016) 93–98.
[30] M. Nasrollahzadeha, M. Ataroda, S.M. Sajadi, Green synthesis of the Cu/Fe_3O_4 nano particles using Morindamorindoides leaf aqueous extract: A highly efficient magnetically separable catalyst for the reduction of organic dyes in aqueous medium at room temperature. Appl. Surf. Sci., 364 (2016) 636–644.
[31] M. Monier, D.M. Ayad, A. Abdel-Latif, Adsorption of Cu (II), Cd (II) and Ni (II) ions by cross-linked magnetic chitosan-2-aminnopyridine glyoxal Schiff´s base, Colloids Surf., B 94 (2012) 250.
[32] C.F. Carolin, P.S. Kumar, A. Saravanan, G.J. Joshiba, M. Naushad, Efficient techniques for the removal of toxic heavy metals from aquatic environment: A review, J. Env. Chem. Eng., 5 (2017) 2782–2799.
[33] A.A. Alqadami, Mu. Naushad, Z.A. ALOthman, Ayman A. Ghfar, Novel metal–organic framework (MOF) based composite material for the sequestration of U (VI) and Th (IV) metal ions from aqueous environment, ACS Appl. Mat. Interfaces, 9 (2017) 36026–36037.
[34] A. Pugazhendhi, G.M. Boovaragamoorthy, K. Ranganathan, Mu. Naushad, T. Kaliannan, New insight into effective biosorption of lead from aqueous solution using Ralstonia solanacearum: Characterization and mechanism studies, J. Clean. Prod., 174 (2018) 1234–1239.
[35] M. Naushad, T. Ahamad, M. Basheer, Al-Maswari, A.A. Alqadami, S.M. Alshehri, Nickel ferrite bearing nitrogen-doped mesoporous carbon as efficient adsorbent for the removal of highly toxic metal ion from aqueous medium, Chem. Eng. J., 330 (2017) 1351–1360.
[36] M. Naushad, Z.A. Alothman, Separation of toxic Pb^{2+} metal from aqueous solution using strongly acidic cation-exchange resin: analytical applications for the removal of metal ions from pharmaceutical formulation, Desal. Water Treat., 53 (2015) 2158–2166.
[37] A. Mittal, M. Naushad, G. Sharma, Z.A. ALothman, S.M. Wabaidur, Fabrication of MWCNTs/ThO_2 nano composite and its adsorption behavior for the removal of Pb (II) metal from aqueous medium, Desal. Water Treat., 57 (2016) 21863–21869.
[38] M.A. Hashim, S. Mukhopadhyay, J.N. Sahu, B. Sengupta, Remediation technologies for heavy metal contaminated groundwater, J. Environ. Manage., 92(10) (2011) 2355.
[39] M. Naushad, S. Vasudeva, G. Sharma, A. Kumar, Z.A. ALOthman, Adsorption kinetics, isotherms and thermodynamic studies for Hg^{2+} adsorption from aqueous medium using alizarin red-SloadedamberliteIRA-400resin, Desal. Water Treat., 57 (2016) 18551–18559.
[40] T.A.Rangreez, A.M. Asiri, B.G. Alhogbi, M. Naushad, Synthesis and ion-exchange properties of graphene Th (IV) phosphate composite cation exchanger: its applications in the selective separation of lead metal ions, Int. J. Env. Res. Public Health A14 (2017) 828–838.
[41] R. Bushra, M. Naushad, G. Sharma, Z.A. ALOthman, A. Azam, Synthesis of polyaniline based composite material and its analytical applications for the removal of highly toxic Hg^{2+} metal ion: antibacterial activity against E.coli, Korean J. Chem. Eng. 34 (2017) 1970–1979.
[42] S.H. Jang, B.G. Min, Y.G. Jeong, W.S. Lyoo, S.C. Lee, Removal of lead ions in aqueous solution by hydroxyapatite/polyurethane composite foams, J. Hazard. Mater., 152 (2008) 1285–1292.
[43] J. Ni, L. Xiong, C. Chen, Q. Chen, Adsorption of Pb (II) and Cd (II) from aqueous solutions using titanate nano tubes prepared via hydrothermal method, J. Hazard. Mater., 189 (2011) 741–748.
[44] A. Selatnia, A. Boukazoula, N. Kechid, M.Z. Bakhti, A. Chergui, Y. Kerchich, Bio sorption of lead (II) from aqueous solution by a bacterial dead Streptomyces rimosus biomass, Biochem. Eng. J., 19 (2004) 127–135.
[45] F. Shah, T.G. Kazi, H.I. Afridi, S. Khan, N.F. Kolachi, M.B. Arain, J.A. Baig, The influence of environmental exposure on lead concentrations in scalp hair of children in Pakistan, Ecotoxicol. Environ. Saf., 74 (2011) 727–732.
[46] A. Alqadmi, Mu. Naushad, T. Ahamd, M.A. Abdalla, Z.A. ALOthman, S.M. AlShehri, Synthesis and characterization of Fe_3O_4@TSC nano composite: Highly efficient removal of toxic metal ions from aqueous medium, RSC Adv 6 (2016) 22679–22689.
[47] S. Venkateswarlu, B.N. Kumar, C. Prasad, P. Venkateswarlu, N.V.V. Jyothi, Bio-inspired green synthesis of Fe_3O_4 spherical magnetic nano particles using Syzygiumcumini seed extract. Physica. B., 449 (2014) 67–71.
[48] C.H. Weng, Modeling Pb (II) adsorption onto sandy loam soil Chih-Huang Weng, J. Colloid Interface Sci., 272 (2004) 262–270.
[49] S. Yang, J. Hu, C. Chen, D. Shao, X. Wang, Mutual Effcts of Pb (II) and humic acid adsorption on multi walled carbon nano tubes/polyacrylamide composites from aqueous solutions, Environ. Sci. Technol., 45 (2011) 3621–3627.
[50] S. Lagergren, About the theory of so called adsorption of soluble substances, KungligaSvenskaVetenskapsakademiens, Handlingar, Band, 24 (1898) 1–39.
[51] Y.S. Ho, G. Mckay, Pseudo-second order model for sorption processes, Process Biochem., 34 (1999) 451–465.
[52] I. Langmuir, The adsorption of gases on plane surfaces of glass, mica and platinum, J. Am. Chem. Soc., 40 (1918) 1361–1403.
[53] H.M.F. Freundlich, Over the adsorption in solution, J. Phys. Chem., 57 (1906) 385–470.
[54] J. Liu, T. Mwamulima, Y. Wang, Y. Fang, S. Song, C. Peng, Removal of Pb (II) and Cr (VI) from aqueous solutions using the fly ash-based adsorbent material-supported zero-valent iron, J. Molec. Liq., 243 (2017) 205–211.
[55] L. Fan, C. Luo, M. Sun, X. Li, H. Qiu, Highly selective adsorption of lead ions by water-dispersible magnetic chitosan/graphene oxide composites, Colloids Surf. B., 103 (2013) 523–529.
[56] T. Depci, Comparison of activated carbon and iron impregnated activated carbon derived from Golbag lignite to remove cyanide from water, Chem. Eng. J., 181 (2012) 467–478.
[57] B. Kakavandi, R. RezaeiKalantary, A. JonidiJafari, S. Nasseri, A. Ameri, A. Esrafili, A. Azari, Pb (II) adsorption onto a magnetic composite of activated carbon and super paramagnetic Fe_3O_4 nano particles: experimental and modeling study, Clean Soil Air Water, 43 (2015) 1157–1166.
[58] M. Mahdavi, M.B. Ahmad, M.J. Haron, Y. Gharayebi, K. Shameli, B. Nadi, Fabrication and characterization of SiO_2/(3-aminopropyl) triethoxysilane-coated magnetite nano particles for lead (II) removal from aqueous solution. J. Inorg. Organomet. Polym., 23 (2013) 599–607.
[59] M. Kumari, C.U. Pittman, D. Mohan, Heavy metals [chromium (VI) and lead (II)] removal from water using mesoporous magnetite (Fe_3O_4) nano spheres, J. Colloid Interface Sci., 442 (2015) 120–132.
[60] W.S.W. Ngah, S. Fatinathan, Adsorption characterization of Pb (II) and Cu (II) ions onto chitosan-tripoly phosphate beads: kinetic, equilibrium and thermodynamic studies, J. Environ. Manage., 91 (2010) 958–969.
[61] C.M. Futalan, C.C. Kan, M.L. Dalida, K.J. Hsien, C. Pascuad, M.W. Wan, Comparative and competitive adsorption of copper, lead, and nickel using chitosan immobilized on bentonite, Carbohyd. Polym., 83 (2011) 52–536.

[62] M. Naushad, Z.A. ALOthman, M.R. Awual, M.M. Alam, G.E. Eldesoky, Adsorption kinetics, isotherms, and thermodynamic studies for the adsorption of Pb^{2+} and Hg^{2+} metal ions from aqueous medium using Ti (IV) iodovanadate cation exchanger, Ionics, 21 (2015)2237–2245.
[63] M. Naushad, Z.A. ALOthman, Inamuddin, H. Javadian, Removal of Pb (II) from aqueous solution using ethylene diamine tetra acetic acid-Zr (IV) iodate composite cation exchanger: Kinetics, isotherms and thermodynamic studies, J. Ind. Eng. Chem., 25 (2015) 35–41.
[64] R. Bushra, Mu. Naushad, R. Adnan, Z.A. ALOthman, M. Rafatullah, Polyaniline supported nano composite cation exchanger: Synthesis, characterization and applications for the efficient removal of Pb^{2+} ion from aqueous medium, J. Ind. Eng. Chem., 21 (2015) 1112–1118.
[65] M. Naushad, Surfactant assisted nano-composite catione x changer: Development, characterization and applications for the removal of toxic Pb^{2+} from aqueous medium, Chem. Eng. J., 235 (2014) 100–108.